LETTER

doi:10.1038/nature14342

Measurement of the first ionization potential of lawrencium, element 103

T. K. Sato[1], M. Asai[1], A. Borschevsky[2,3], T. Stora[4], N. Sato[1], Y. Kaneya[1,5], K. Tsukada[1], Ch. E. Düllmann[3,6,7], K. Eberhardt[3,7], E. Eliav[8], S. Ichikawa[1,9], U. Kaldor[8], J. V. Kratz[7], S. Miyashita[10], Y. Nagame[1,5], K. Ooe[11], A. Osa[1], D. Renisch[7], J. Runke[6], M. Schädel[1], P. Thörle-Pospiech[3,7], A. Toyoshima[1] & N. Trautmann[7]

The chemical properties of an element are primarily governed by the configuration of electrons in the valence shell. Relativistic effects influence the electronic structure of heavy elements in the sixth row of the periodic table, and these effects increase dramatically in the seventh row—including the actinides—even affecting ground-state configurations[1,2]. Atomic *s* and $p_{1/2}$ orbitals are stabilized by relativistic effects, whereas $p_{3/2}$, *d* and *f* orbitals are destabilized, so that ground-state configurations of heavy elements may differ from those of lighter elements in the same group. The first ionization potential (IP_1) is a measure of the energy required to remove one valence electron from a neutral atom, and is an atomic property that reflects the outermost electronic configuration. Precise and accurate experimental determination of IP_1 gives information on the binding energy of valence electrons, and also, therefore, on the degree of relativistic stabilization. However, such measurements are hampered by the difficulty in obtaining the heaviest elements on scales of more than one atom at a time[3–5]. Here we report that the experimentally obtained IP_1 of the heaviest actinide, lawrencium (Lr, atomic number 103), is $4.96^{+0.08}_{-0.07}$ electronvolts. The IP_1 of Lr was measured with ^{256}Lr (half-life 27 seconds) using an efficient surface ion-source and a radioisotope detection system coupled to a mass separator. The measured IP_1 is in excellent agreement with the value of 4.963(15) electronvolts predicted here by state-of-the-art relativistic calculations. The present work provides a reliable benchmark for theoretical calculations and also opens the way for IP_1 measurements of superheavy elements (that is, transactinides) on an atom-at-a-time scale.

The chemical characterization of heavy elements at the end of the actinides and of all transactinides, performed to probe their positions in the periodic table[4–10], has been, so far, conducted by rapid chemical separation techniques, such as gas-phase and liquid-phase chromatography. The influence of relativistic effects on electronic orbitals has been inferred indirectly, through a comparison of the chemical properties of the heavy elements with those of their lighter homologues and those predicted by theoretical calculations. The first ionization potential, one of the most fundamental physical and chemical properties of an element, gives direct information about the binding energy of an electron in the outermost electronic orbital of an atom. Accurate IP_1 values of heavy elements provide crucial tests for our understanding of their electronic structure. IP_1 values of weighable amounts of nuclear-reactor-produced heavy elements up to einsteinium (atomic number $Z = 99$) have been successfully measured by resonance ionization mass spectroscopy (RIMS)[11,12]. RIMS was also used in an investigation of fermium (Fm, $Z = 100$) with a sample of 2.7×10^{10} atoms of ^{255}Fm (half-life $T_{1/2} = 20.1$ h). In that experiment, the atomic level structure, but not the IP_1, was determined[13]. Recently, resonance ionization laser ion source (RILIS) studies optimized for short-lived atoms made it possible to determine the IP_1 of astatine (At, $Z = 85$) using ^{199}At ($T_{1/2} = 7.2$ s) produced in the proton-induced spallation reaction of uranium[14]. IP_1 values of heavy elements with $Z \geq 100$, however, could not be determined experimentally, because production rates drastically decrease for elements as their atomic number increases. The study of these elements therefore requires new techniques, on an atom-at-a-time scale.

The ground-state electronic configuration of Lr is predicted to be $[Rn]5f^{14}7s^27p_{1/2}$, in contrast to that of its lanthanide homologue Lu, $[Xe]4f^{14}6s^25d$, as the $7p_{1/2}$ orbital is expected to be stabilized below the $6d$ orbital in Lr by strong relativistic effects[15–19]. The determination of IP_1 sheds light on the important role of relativistic effects in heavy elements by comparison with theoretical predictions. For Lr, theory predicts an exceptionally low IP_1 value. A sufficiently long-lived and detectable isotope for ionization experiments is ^{256}Lr ($T_{1/2} = 27$ s). It is produced at a rate of one atom per several seconds in the fusion-evaporation reaction of a ^{249}Cf target with a ^{11}B beam[20]. With this constraint, a new and highly efficient experimental set-up based on the ionization and detection of the $^{256}Lr^+$ ion has been devised and implemented to determine the IP_1 value of Lr.

The surface ionization process takes place on a solid surface kept at high temperature, which is coupled to an on-line mass separator; that is, an atom is ionized to the 1+ charge state via the interaction with a solid (metal) surface at high temperature and is selectively mass-separated from nuclear reaction by-products. Figure 1 depicts the experimental set-up schematically. Short-lived ^{256}Lr atoms recoiling off a ^{249}Cf target were promptly transported to the ionization site (ionization cavity) by He/CdI_2 gas-jet transport, and surface-ionized ^{256}Lr atoms were extracted and mass-separated. The number of ^{256}Lr ions after the mass-separation was determined by α-particle spectroscopy. Experimental details are provided in the Methods section and in ref. 20.

Based on the Saha-Langmuir equation[21,22], an analytical model[23] describes the surface ionization process in a hollow tube (cavity)-type ion-source. The ionization efficiency I_{eff} can be expressed as:

$$I_{eff} = \frac{N\exp\left(\frac{\phi - IP_1^*}{kT}\right)}{1 + N\exp\left(\frac{\phi - IP_1^*}{kT}\right)} \quad (1)$$

where ϕ is the work function, which is material-dependent, k the Boltzmann constant, T the temperature of the ionizing surface, and N a parameter that depends on the effective number of atom–surface interactions in the cavity. IP_1*, the effective IP_1, is directly related to IP_1 as[22]:

$$IP_1^* = IP_1 - kT\ln\left(\frac{Q_i}{Q_0}\right) \quad (2)$$

where Q_i and Q_0 are the partition functions at a given temperature for the ion and the atom, respectively, which can be calculated using excitation

[1]Japan Atomic Energy Agency (JAEA), Tokai, Ibaraki 319-1195, Japan. [2]Centre for Theoretical Chemistry and Physics, New Zealand Institute for Advanced Study, Massey University, 0745 North Shore MSC, Auckland, New Zealand. [3]Helmholtz-Institut Mainz, 55099 Mainz, Germany. [4]ISOLDE, CERN, CH-1211 Geneva 23, Switzerland. [5]Graduate School of Science and Engineering, Ibaraki University, Mito, Ibaraki 310-8512, Japan. [6]GSI Helmholtzzentrum für Schwerionenforschung, 64291 Darmstadt, Germany. [7]Institut für Kernchemie, Johannes Gutenberg-Universität Mainz, 55099 Mainz, Germany. [8]School of Chemistry, Tel Aviv University, 69978 Tel Aviv, Israel. [9]Nishina Center for Accelerator-Based Science, RIKEN, 2-1 Hirosawa, Wako, Saitama 351-0198, Japan. [10]Graduate School of Science, Hiroshima University, Kagamiyama, Higashi-Hiroshima 739-8526, Japan. [11]Institute of Science and Technology, Niigata University, Niigata 910-2181, Japan.

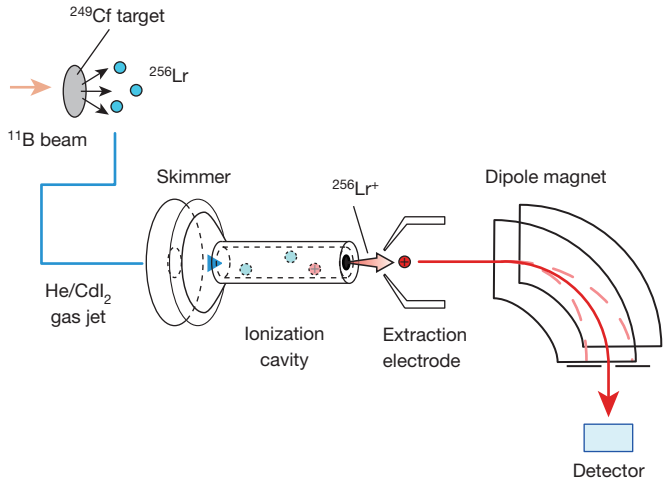

Figure 1 | Schematic experimental set-up used to measure the IP_1 of Lr on an atom-at-a-time scale. ^{256}Lr atoms produced in the nuclear reaction ^{249}Cf(^{11}B, 4n) are transported (blue line) by the He/CdI_2 gas jet to a tantalum ionization cavity via a skimmer component. The ^{256}Lr atoms are ionized on the tantalum surface. The $^{256}Lr^+$ ions produced are extracted electrostatically from the cavity by the extraction electrode, accelerated by 30 kV, and mass-separated by a dipole magnet. See Methods for details. The number of mass-separated $^{256}Lr^+$ ions is determined by α-particle spectroscopy at the detector position.

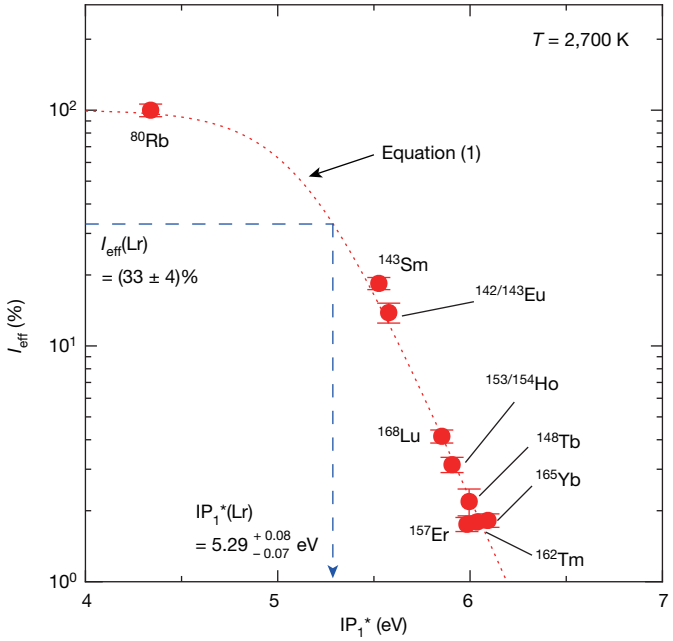

Figure 2 | The ionization efficiency (I_{eff}) of various short-lived isotopes as a function of the effective IP_1 (IP_1*) at 2,700 K. The short-dashed curve is obtained by fitting the experimental data using equation (1), which describes a relationship between I_{eff} and IP_1* in our present system. The position of the measured I_{eff} value of Lr, (33 ± 4)%, is also shown. From the fitted equation (1) with $N = 43 \pm 3$, IP_1* of Lr is calculated to be $5.29^{+0.08}_{-0.07}$ eV. This corresponds to an IP_1 value of $4.95^{+0.10}_{-0.08}$ eV at 2,700 K. Error bars, ±1s.d.

energies and statistical weights of their ground and excited states. Tantalum (Ta) was chosen as the cavity material. The ionization experiments were conducted at $T = 2{,}700$ K and 2,800 K. For ^{256}Lr, I_{eff} values of (33 ± 4)% and (36 ± 7)%, respectively, were determined by the procedure given in ref. 20.

The following procedure was applied to determine the value of the free parameter N in equation (1): short-lived lanthanide and alkali isotopes ^{142,143}Eu, ^{143}Sm, ^{148}Tb, ^{153,154}Ho, ^{157}Er, ^{162}Tm, ^{165}Yb, ^{168}Lu and ^{80}Rb were produced in nuclear reactions of ^{11}B beams with target materials of ^{136}Ce, ^{141}Pr, ^{142}Nd, ^{147}Sm, Eu, ^{156}Gd, ^{159}Tb, ^{162}Dy and Ge, respectively, and their I_{eff} values were experimentally determined at $T = 2{,}700$ K and 2,800 K. Figure 2 shows the I_{eff} values at 2,700 K as a function of IP_1*. The IP_1* value for each element was calculated with equation (2). Energies and statistical weights of low-lying states in the ion and the atom of each element were taken from the National Institute of Standards and Technology (NIST) atomic database[24]. The I_{eff} values determined for all isotopes were best fitted with equation (1) using N values of 43 ± 3 and 50 ± 3 at $T = 2{,}700$ K and 2,800 K, respectively.

The Lr IP_1* values of $5.29^{+0.08}_{-0.07}$ eV and $5.33^{+0.11}_{-0.10}$ eV were determined from equation (1) at $T = 2{,}700$ K and 2,800 K, respectively. The result at 2,700 K is illustrated in Fig. 2. Errors on the IP_1* values mainly came from three sources of uncertainty: surface temperatures, I_{eff} (which is based on counting statistics) and fitting procedures. The Lr IP_1 can be calculated from IP_1* using equation (2) with Q_i and Q_0. No experimental data on excited states of the Lr atom and ion are available. Thus, the energies and statistical weights for calculating Q_i and Q_0 were taken from relativistic Fock space coupled cluster (FSCC) calculations[18]. The average absolute error for the 20 lowest excitation energies of Lu (where comparison with experiment is possible) was 0.05 eV using the same approach[18]. We expected a similar accuracy for the predicted transition energies of Lr. The evaluated values of $kT\ln(Q_i/Q_0)$ for Lr at $T = 2{,}700$ K and 2,800 K are $-0.34^{+0.06}_{-0.04}$ and $-0.36^{+0.06}_{-0.04}$, respectively. The errors include uncertainties in the calculated excitation energies indicated in ref. 18, 0.087 eV (700 cm^{-1}) for each state, and in the temperatures. From this, IP_1 values of $4.95^{+0.10}_{-0.08}$ eV and $4.97^{+0.13}_{-0.11}$ eV were obtained at $T = 2{,}700$ K and 2,800 K, respectively. Based on these results, our experimentally determined value for IP_1 of Lr is $4.96^{+0.08}_{-0.07}$ eV.

A theoretical calculation of the IP_1 of Lr was also performed, using the relativistic coupled cluster approach with single, double, and perturbative triple excitations (DC CCSD(T)), and corrected for the Breit contribution and Lamb shift (Methods). The calculated $7s^27p_{1/2}$ level of Lr is lower by ~180 meV than $7s^26d_{3/2}$, confirming earlier identification of the former as the atomic ground state. This is due to relativistic effects; a non-relativistic calculation puts the energy of the $7s^26d$ configuration about 2.2 eV below that of $7s^27p$. To assess the accuracy of our predicted IP_1 of Lr, the same approach was applied to its lighter homologue Lu. The calculated ground state of the latter is experimentally confirmed as $6s^25d$. The Lr^+ ion has a closed-shell $[Rn]5f^{14}7s^2$ ground-state configuration. The IP_1 was obtained by taking the difference between the calculated energies of the neutral state and the 1+ state. The calculated IP_1 values are 5.418 eV for Lu and 4.963 eV for Lr. Corrections for the Breit contribution were 6 meV for Lu and −12 meV for Lr, and corrections for the Lamb shift were 0.3 meV for Lu and 16 meV for Lr (ref. 25). The calculated IP_1 for Lu is in very good agreement with the experimental IP_1 of 5.425871(12) eV (ref. 26); similar accuracy is expected for the calculated IP_1 of Lr.

The experimental and calculated IP_1 results obtained in our work are shown in Table 1 together with earlier theoretical predictions. It should be noted that the calculated excitation energies of Lr, which we used to

Table 1 | Theoretical and experimental IP_1 values of Lr

Reference	Year	IP_1 (eV)	Method
Ref. 16	1995	4.887	DCB+FSCC*
Ref. 27	1998	5.28	RECP+CASSCF+ACPF+Δ_{SO}†
Ref. 28	2003	4.80	RECP+CASSCF+ACPF+Δ_{SO}†
Ref. 18	2007	4.893	DCB+FSCC*
Ref. 19	2014	4.934	CI+all-order‡
This work		4.963(15)	DC CCSD(T)+Breit+Lamb shift§
This work		$4.96^{+0.08}_{-0.07}$	Experimental

*Dirac Coulomb Breit (DCB) Hamiltonian combined with the Fock space coupled cluster (FSCC) approach.
†Relativistic effective core potentials (RECP) combined with complete active space multiconfiguration self-consistent field (CASSCF) calculations with subsequent multi-reference averaged coupled-pair functional (ACPF) calculations and spin orbit corrections (Δ_{SO}).
‡Configuration interaction (CI) method combined with the linearized single-double coupled cluster method (all-order).
§Dirac Coulomb (DC) Hamiltonian combined with CCSD(T) approach and corrected for the Breit contribution and the Lamb shift.

get Q_i and Q_0 values to derive the experimental IP_1 from IP_1*, were obtained with a method different to the one employed here for the calculation of the IP_1 itself. As the two calculations are independent, we can compare the present experimental and theoretical IP_1 values. Our experimental result on the first ionization potential of Lr of $4.96^{+0.08}_{-0.07}$ eV is in excellent agreement with the theoretical value of 4.963(15) eV also obtained in this work.

Thus, we have experimentally shown that the IP_1 of Lr is distinctly lower than that of Lu. Lr, the heaviest actinide, has the lowest IP_1 value of all lanthanides and actinides; this quantitatively reflects and confirms the theoretically predicted situation of closed $5f^{14}$ and $7s^2$ shells with an additional weakly-bound electron in the valence orbital. We note that the surface ionization method, successfully applied here to determine the IP_1 of Lr, can provide experimental data that can benchmark quantum chemical calculations of the heaviest elements. In addition, it opens up new perspectives on determining basic atomic properties of the superheavy elements.

Online Content Methods, along with any additional Extended Data display items and Source Data, are available in the online version of the paper; references unique to these sections appear only in the online paper.

Received 27 November 2014; accepted 6 February 2015.

1. Pyykkö, P. Relativistic effects in structural chemistry. *Chem. Rev.* **88,** 563–594 (1988).
2. Pershina, V. in *Relativistic Methods for Chemists* (eds Barysz, M. & Ishikawa, Y.) 451–520 (Challenges and Advances in Computational Chemistry and Physics 10, Springer, 2010).
3. Oganessian, Yu. Heaviest nuclei from ^{48}Ca-induced reactions. *J. Phys. G* **34,** R165–R242 (2007).
4. Schädel, M. & Shaughnessy, D. (eds) *The Chemistry of Superheavy Elements* 2nd edn (Springer, 2014).
5. Türler, A. & Pershina, V. Advances in the production and chemistry of the heaviest elements. *Chem. Rev.* **113,** 1237–1312 (2013).
6. Schädel, M. *et al.* Chemical properties of element 106 (seaborgium). *Nature* **388,** 55–57 (1997).
7. Eichler, R. *et al.* Chemical characterization of bohrium (element 107). *Nature* **407,** 63–65 (2000).
8. Düllmann, Ch. E. *et al.* Chemical investigation of hassium (element 108). *Nature* **418,** 859–862 (2002).
9. Eichler, R. *et al.* Chemical characterization of element 112. *Nature* **447,** 72–75 (2007).
10. Even, J. *et al.* Synthesis and detection of a seaborgium carbonyl complex. *Science* **345,** 1491–1493 (2014).
11. Köhler, S. *et al.* First experimental determination of the ionization potentials of berkelium and californium. *Angew. Chem. Int. Edn Engl.* **35,** 2856–2858 (1996).
12. Peterson, J. *et al.* Determination of the first ionization potential of einsteinium by resonance ionization mass spectroscopy (RIMS). *J. Alloy. Comp.* **271–273,** 876–878 (1998).
13. Sewtz, M. *et al.* First observation of atomic levels for the element fermium (Z = 100). *Phys. Rev. Lett.* **90,** 163002 (2003).
14. Rothe, S. *et al.* Measurement of the first ionization potential of astatine by laser ionization spectroscopy. *Nature Commun.* **4,** 1835 (2013).
15. Desclaux, J.-P. & Fricke, B. Relativistic prediction of the ground state of atomic lawrencium. *J. Phys.* **41,** 943–946 (1980).
16. Eliav, E., Kaldor, U. & Ishikawa, Y. Transition energies of ytterbium, lutetium, and lawrencium by the relativistic coupled-cluster method. *Phys. Rev. A* **52,** 291–296 (1995).
17. Zou, Y. & Fischer, C. F. Resonance transition energies and oscillator strengths in lutetium and lawrencium. *Phys. Rev. Lett.* **88,** 183001 (2002).
18. Borschevsky, A. *et al.* Transition energies of atomic lawrencium. *Eur. Phys. J. D* **45,** 115–119 (2007).
19. Dzuba, V. A., Safronova, M. S. & Safronova, U. I. Atomic properties of superheavy elements No, Lr, and Rf. *Phys. Rev. A* **90,** 012504 (2014).
20. Sato, T. K. *et al.* First successful ionization of Lr (Z = 103) by a surface-ionization technique. *Rev. Sci. Instrum.* **84,** 023304(5) (2013).
21. Stora, T. *Radioactive Ion Sources.* CERN-2013-007, 331–349 http://cds.cern.ch/record/1693046 (accessed November 2014).
22. Zandberg, É. Y. & Ionov, N. I. Surface ionization. *Sov. Phys. Usp.* **2,** 255–281 (1959).
23. Kirchner, R. On the thermoionization in hot cavities. *Nucl. Instrum. Methods A* **292,** 203–208 (1990).
24. Kramida, A., Ralchenko, Y., Reader, J. & Team, N. A. *NIST Atomic Spectra Database* version 5.1 (2013); http://physics.nist.gov/asd (accessed July 2014).
25. Shabaev, V. M., Tupitsyn, I. I. & Yerokhin, V. A. QEDMOD: Fortran program for calculating the model Lamb-shift operator. *Comput. Phys. Commun.* **189,** 175–181 (2015).
26. Maeda, H., Mizugai, Y., Matsumoto, Y., Suzuki, A. & Takami, M. Highly excited even Rydberg series of Lu I studied by two-step laser photoionization spectroscopy. *J. Phys. B* **22,** L511–L516 (1989).
27. Liu, W., Küchle, W. & Dolg, M. *Ab initio* pseudopotential and density-functional all-electron study of ionization and excitation energies of actinide atoms. *Phys. Rev. A* **58,** 1103–1110 (1998).
28. Cao, X., Dolg, M. & Stoll, H. Valence basis sets for relativistic energy-consistent small-core actinide pseudopotentials. *J. Chem. Phys.* **118,** 487–496 (2003).

Acknowledgements We thank the JAEA tandem accelerator crew for supplying intense and stable beams for the experiments. The ^{249}Cf was made available by H. Nitsche (Univ. California, Berkeley); it was produced in the form of ^{249}Bk through the former Transplutonium Element Production Program at Oak Ridge National Laboratory (ORNL) under the auspices of the Director, Office of Science, Office of Basic Energy Sciences, Chemical Sciences, Geosciences, and Biosciences Division of the US Department of Energy. Financial support by the Helmholtz-Institut Mainz is acknowledged. This work has been partly supported by the Grant-in-Aid for Scientific Research (C) no. 26390119 of the Ministry of Education, Science, Sports and Culture (MEXT).

Author Contributions T.K.S., M.A., Y.N. and M.S. prepared the main part of the manuscript, A.B., E. E. and U.K. contributed to the theory part, and T.S. to the experimental part. C.E.D. and J.V.K. commented on the manuscript. T.K.S, M.A., T.S., N.S., K.T. and S.I. developed the surface ion-source in the ISOL setup at the JAEA tandem accelerator facility. T.K.S. and M.A. were responsible for data acquisition and analysis. T.S. commented on ion-source optimizations and the data analysis procedure. K.T. prepared the ^{249}Cf target. K.E., J.R., P.T.-P., C.E.D. and N.T. separated and provided the ^{249}Cf for the target. The on-line experiments were performed by T.K.S., M.A., N.S., Y.K., K.T., S. I., S.M., Y.N., K.O., A.O., D.R., M.S. and A.T., while theoretical calculations were carried out by A.B., E.E. and U.K. All authors discussed the results and commented on the manuscript.

Author Information Reprints and permissions information is available at www.nature.com/reprints. The authors declare no competing financial interests. Readers are welcome to comment on the online version of the paper. Correspondence and requests for materials should be addressed to Y.N. (nagame.yuichiro@jaea.go.jp).

METHODS

Ionization experiments. The set-up consists of a target-recoil chamber coupled to an aerosol gas-jet transport system, a surface ion-source, a mass separator, and a detection system for nuclear decays[20]. For the Lr experiment, a ^{249}Cf target (thickness 260 μg cm^{-2}) in the target-recoil chamber was irradiated with a 67.9-MeV $^{11}B^{4+}$ beam delivered from the Tandem accelerator at the Japan Atomic Energy Agency (JAEA), Tokai[20,29]. ^{256}Lr atoms, recoiling from the target, attached onto CdI_2 particles produced by sublimation of CdI_2, were transported to the ionization cavity of the ion-source installed in the Isotope Separator On-Line (JAEA-ISOL)[20,30]. Before entering the ionization cavity, aerosol particles with the attached ^{256}Lr passed through a skimmer structure, installed to remove the He carrier gas to achieve high vacuum conditions at the ion-source (typically 2×10^{-2} Pa). In the cavity, the aerosol particles were vaporized and ^{256}Lr atoms were surface ionized. The temperature of the cavity was monitored with a calibrated radiation thermometer with ±50 K accuracy. The cavity can be heated up to 2,850 K. Ions were extracted and accelerated by an electrostatic potential of 30 kV. $^{256}Lr^{+}$ ions were mass separated in the dipole magnet of the JAEA-ISOL and were transported to the detection device. The nuclear decay of ^{256}Lr was measured with eight pairs of Si PIN photodiodes of a rotating catcher wheel apparatus, MANON (Measurement system of Alpha particle and spontaneous fissioN events ON-line) for efficient α-particle measurements[20].

For the short-lived isotope experiments to obtain a relationship between I_{eff} and IP_1* in the present system, various isotopes, ^{142,143}Eu, ^{143}Sm, ^{148}Tb, ^{153,154}Ho, ^{157}Er, ^{162}Tm, ^{165}Yb, ^{168}Lu and ^{80}Rb, were employed. These isotopes were produced in reactions of ^{11}B with targets consisting of ^{136}Ce, ^{141}Pr, ^{142}Nd, ^{147}Sm, Eu, ^{156}Gd, ^{159}Tb, ^{162}Dy and Ge, respectively. Mass-separated ions were collected on an aluminized Mylar tape in a tape transport system installed between the end of the ISOL beam line and the MANON set-up[20]. A high-purity germanium (HP-Ge) detector was placed at the tape transport system to determine the number of the ions by γ spectroscopy.

Calculation of I_{eff} and IP_1*. To calculate the I_{eff} value of each isotope, the number of atoms transported to the ion-source was determined by a direct-catch measurement. Nuclear reaction products were directly collected at a separate collection site where their radioactivity was measured before the ISOL experiments. Here, the measurement of ^{256}Lr was performed using another MANON set-up. For the measurements of the other isotopes, aerosol particles from the target recoil chamber were collected on a glass fibre filter. The γ-rays of each isotope on the glass fibre filter were measured using a HP-Ge detector. Because of the low IP_1 of Rb, it is justified to assume that the I_{eff} of ^{80}Rb should be 100% in the surface ionization. By using ^{80}Rb as a reference material, I_{eff} of the other elements were calculated[20].

For a calculation of IP_1*, equation (2) is applied to each element. Q_i and Q_0 in equation (2) are described as follows[22],

$$\begin{cases} Q_i = \sum_j g_i^j \exp\left(-\dfrac{E_i^j}{kT}\right) \\ Q_0 = \sum_j g_0^j \exp\left(-\dfrac{E_0^j}{kT}\right) \end{cases} \quad (3)$$

where g_i^j and g_0^j are the statistical weights of the jth quantum state of the ion and the atom, respectively. The $j = 0$ corresponds to the ground state. Here, E_i^j and E_0^j are the energies of excitation to the jth quantum state of the ion and the atom, respectively. Excited states whose excitation energy is much higher than kT can be neglected because $\exp\left(-\dfrac{E}{kT}\right)$ is approaching zero. Using equations (3), Q_i and Q_0 values were calculated. Applying these results to the IP_1* value for each element, the IP_1 value was calculated by equation (2).

Theoretical calculation. The CCSD(T) calculations of the IP_1 of Lu and Lr were carried out using the DIRAC13 computational program package[31], in the framework of the relativistic Dirac-Coulomb Hamiltonian. The IP_1 was obtained as the difference between the calculated energies of the neutral and mono-cation species. The Faegri dual family basis sets of uncontracted Gaussian-type orbitals[32] were used. These sets were augmented by high angular momentum and diffuse functions up to convergence of the calculated IP_1 values. The final basis sets consist of 25*s* 23*p* 15*d* 14*f* 6*g* 3*h* orbitals for Lu and 27*s* 25*p* 17*d* 14*f* 6*g* 3*h* 2*i* orbitals for Lr. The finite nucleus model with Gaussian charge distribution was used[33].

Effects of higher-order terms of the Hamiltonian on the IP_1 values, namely the frequency independent Breit operator and the Lamb shift, were also calculated. These terms are not implemented in the DIRAC13 program; the Breit term was therefore calculated using the TRAFS-3C (Tel-Aviv Relativistic Atomic Fock Space coupled cluster code) package[34], and the Lamb energy shift was obtained by the recently developed effective potential method, implemented in the QEDMOD program[25]. The contributions of the Breit term were 6 meV for Lu and −12 meV for Lr; the effect of the Lamb shift on the IP was −0.3 meV for Lu and 16 meV for Lr. These contributions were added to the CCSD(T) results obtained using the DIRAC13 program.

Sample size. No statistical methods were used to predetermine sample size.

29. Sato, N. *et al.* Production of ^{256}Lr in the ^{249,250,251}Cf + ^{11}B, ^{243}Am + ^{18}O, and ^{248}Cm + ^{14}N reactions. *Radiochim. Acta* **102,** 211–219 (2014).
30. Sato, T. K. *et al.* Development of a He/CdI_2 gas-jet system coupled to a surface-ionization type ion-source in JAEA-ISOL: towards determination of the first ionization potential of Lr (Z = 103). *J. Radioanal. Nucl. Chem.* **303,** 1253–1257 (2015).
31. Visscher, L. *et al.* DIRAC, a relativistic *ab initio* electronic structure program. Release DIRAC13 http://www.diracprogram.org (2013).
32. Faegri, K. Relativistic Gaussian basis sets for the elements K-Uuo. *Theor. Chem. Acc.* **105,** 252–258 (2001).
33. Visscher, L. & Dyall, K. G. Dirac–Fock atomic electronic structure calculations using different nuclear charge distributions. *At. Data Nucl. Data Tables* **67,** 207–224 (1997).
34. Eliav, E., Kaldor, U. & Ishikawa, Y. Open-shell relativistic coupled-cluster method with Dirac-Fock-Breit wave functions: energies of the gold atom and its cation. *Phys. Rev. A* **49,** 1724–1729 (1994).